New types of TLM nodes for the analysis of axially symmetric structures

Sandrick Le Maguer, Michel Ney

New Types of TLM Nodes for the Analysis of Axially Symmetric Structures

Sandrick Le Maguer and Michel M. Ney
Laboratory for Electronics and communication Systems (LEST), UMR CNRS 6616
Ecole Nationale Supérieure des Télécommunications de Bretagne, BP 832, 29285 BREST cedex, FRANCE
FAX: +33 2 98 00 13 43, sandrick.lemaguer@enst-bretagne.fr

I- Introduction

The Transmission Line Matrix (TLM) method is a well-known numerical time-domain technique which has been widely used for solving electromagnetic field problems. Axially symmetric structures are frequently encountered in microwave engineering. For this purpose, a first memory-saving TLM algorithm was developed in the particular case of uniform guiding structures [1]. Based on the classical Symmetrical Condensed Node (SCN) [2], this approach leads to a 1D mesh array using 18 complex voltages. Low memory requirement and simple algorithm make this method a very versatile tool. Extension of this model to general axially symmetric structure (2D mesh array) is not memory competitive compared to other time domain methods as BoR-FDTD [3,4].
In this paper, we propose a new TLM scheme for this type of geometry namely, the Axial Symmetry TLM (AS-TLM). This node is directly deduced from Maxwell's integral equations expressed in the case of body of revolution with the approach proposed by Peña and Ney [4]. The basic cell requires 8 arms and from a TLM point of view, it should be considered as composed of one 2D series node and one 2D parallel node coupled by fields at the center (Figure 1). Three types of nodes are hence proposed: a SCN with 6 stubs and one arm impedance (14 real voltages), an HSCN with 3 stubs and three arm impedances (11 real voltages) and, finally, a Hybrid-Hybrid Node (HHSCN) which is composed of 2 stubs and 4 arm impedances (10 real voltages). The name of the HHSCN comes from the fact that it includes two 2D nodes treated as 2D-Hybrid nodes [6]. Current sources and losses are included in the algorithm straightforwardly. At last, absorbing boundary conditions (ABC) specific to the problem are included in the TLM algorithm.

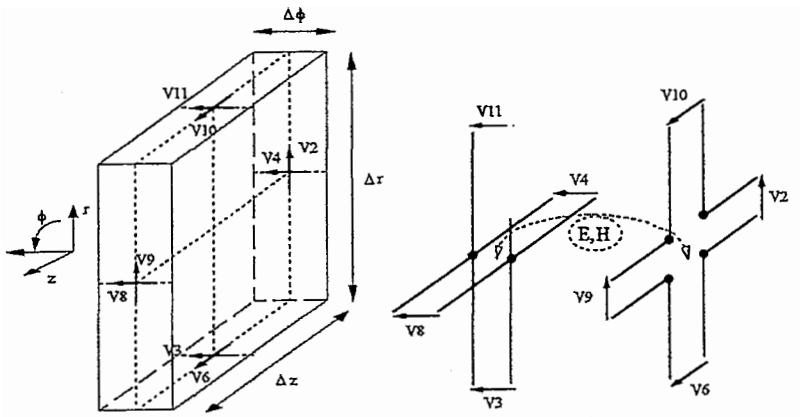

Figure 1 . New TLM node for axially symmetric problems with classical SCN notation **(a)** General aspect of the node **(b)** Its decomposition in two 2D nodes coupled by center fields.

II - Theory

In the new node depicted in Figure 1, only 8 transmission-lines are used, since azimuthal arms are removed. Furthermore, azimuthal dimension, called $\Delta\phi$, is a normalized arbitrary length as shown bellow. It can be chosen to obtain the best time step. With the above dimensions, voltage definition remains the same as in [5] expect for 4 of them:

$$\begin{pmatrix} a_3 \\ a_6 \\ a_{10} \\ a_{11} \end{pmatrix} = \frac{1}{2} \begin{pmatrix} r_1 \Delta\phi\, E_3^{\phi} + Z_{r\phi}\, \Delta z\, H_3^{z} \\ \Delta z\, E_6^{z} - Z_{rz}\, r_1 \Delta\phi\, H_6^{\phi} \\ \Delta z\, E_{10}^{z} + Z_{rz}\, r_2 \Delta\phi\, H_{10}^{\phi} \\ r_2 \Delta\phi\, E_{11}^{\phi} - Z_{r\phi}\, \Delta z\, H_{11}^{z} \end{pmatrix} \quad \text{with:} \quad r_1 = \frac{r - \frac{\Delta r}{2}}{r} \quad \text{and} \quad r_2 = \frac{r + \frac{\Delta r}{2}}{r} \qquad (1)$$

where a indicates incident voltages (b are reflected ones), r is the distance from the center of cylindrical coordinates to the center of the node under consideration and Z_{ij} denote arm impedances. In the case of body of revolution, field Fourier expansion is expressed as follows:

$$\vec{E} = \sum_{m=0}^{\infty} \left(\vec{e}.e^{-jm\phi} \right) \qquad \vec{H} = \sum_{m=0}^{\infty} \left(\vec{h}.e^{-jm\phi} \right) \tag{2}$$

where m is the azimuthal order. Example will be shown for AS-SCN, as AS-HSCN and AS-HHSCN are derived with the same method. Let us consider a (z,ϕ) path integral as depicted in Figure 2. Approximating Maxwell-Ampère integral equation without losses and sources leads to:

$$\frac{(1+T)}{2} 2\sin\left(\frac{m\Delta\phi}{2}\right) e^{-jm\phi_0} \left[\frac{r}{m} \left(H_2^{\phi} - H_9^{\phi} \right) - j\Delta z H_z \right] = (1-T) \frac{\varepsilon_r}{Z_0 c \Delta t} \frac{r \Delta z}{m \Delta r} \Delta r \tilde{E}_r e^{-jm\phi_0} 2\sin\left(\frac{m\Delta\phi}{2}\right) \tag{3}$$

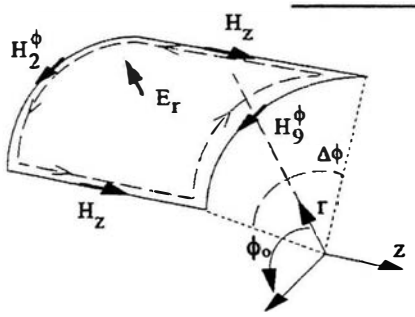

Figure 2 . (z,ϕ) contour path integral for Maxwell equation approximation.

with: $\tilde{E}_r = \dfrac{E_2^r + E_2^r + \hat{Y}_{sr} E_{13}^r}{4 + \hat{Y}_{sr}}$

$$\hat{Y}_{sr} \qquad \frac{\varepsilon_r \Delta\phi \Delta z}{c \Delta t \Delta r} \tag{4}$$

and T is such that $Tu^k = u^{k-1}$.

In a voltage notation, equation (3) is expressed as:

$$b_2 + b_9 + \hat{Y}_{sr}\, b_{13} = a_2 + a_9 + \hat{Y}_{sr}\, a_{13} - \alpha Z_0 \Delta z H_z$$

with $\alpha = j\dfrac{m\Delta\phi}{r}$ (5)

The calculation is then driven for Maxwell-Faraday equation using the same contour path. Thus, the same approximations are made in (r,ϕ) plane and (z,r) plane. Finally, six equations relating incident and reflected voltages are obtained. At this point, the field components at the center of the node are evaluated using the approach proposed in [7] leading, for example, to:

$$\Delta r\, E_r = \frac{2\left(a_2 + a_9 + \hat{Y}_{sr}\, a_{13}\right) - \alpha Z_0 \Delta z H_z}{2 + \hat{Y}_{sr}} \qquad Z_o \Delta z H_z = \frac{2\left(-a_{11} + a_3 + \hat{Z}_{sz}\, a_{18}\right) - \alpha \Delta r E_r}{2 + \hat{Z}_{sz}} \tag{6}$$

One can note that α is a complex constant. Real and imaginary part of field are extracted getting to two independent solutions. One of these is then chosen and kept to perform computation with real variables. For example, real part of E_r, E_z and H_ϕ and imaginary part of H_r, H_z and E_ϕ constitutes one of these solutions. Thus, real and imaginary part of corresponding voltages are used. Finally, reflected voltages are calculated from fields at the center of the node and incident voltages. This part of the algorithm remains unchanged compared to a classical TLM procedure [8]. Furthermore, losses and current sources integration is straightforward as indicated in [5].

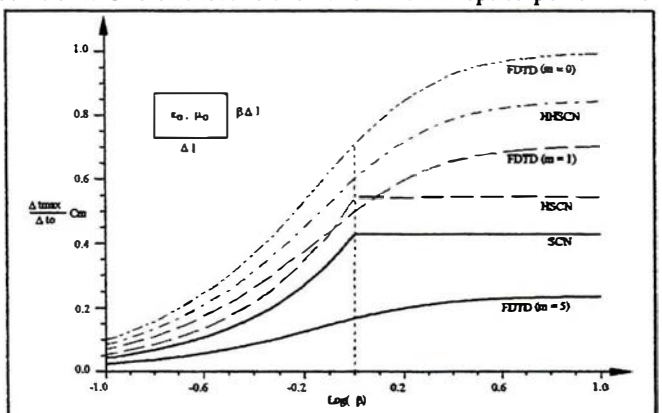

Figure 3 . Normalized maximum time steps (weighted by a term (Cm) taking into account memory requirement) comparison for AS-TLM and BOR-FDTD schemes with cell size variation.

The hybrid node is extracted naturally with the same approach whereas a super condensed node can not be created. To derive a condensed node, 6 degrees of freedom are required. If no stub is used we only have four degrees. An alternative solution is to create an Hybrid-Hybrid node where one stub is associated with each azimuthal field components.

Considering voltages along (o,r) direction, namely V_3, V_6, V_{10} and V_{11}, it should be pointed out that their definition varies from neighboring nodes. As a result, a transfer matrix is used to transfer the voltages along this direction.

The last point of major importance is the treatment of the center of cylindrical coordinates. When the azimuthal order is greater than zero, the longitudinal field components are zero at this location. Hence from (1), it can be seen that the voltages V_3 and V_6 are zero. This implies they are ignored in the equations governing the cell adjacent to the center of coordinates. In the particular case where the azimuthal order is zero, a special cell has to be created for the center. It is obtained by enforcing Maxwell integral equations around the center. It leads to a two-port node with half size in the radial direction, referred to "half node".
Finally, since the maximum time-step is independent of the azimuthal order m, AS-TLM seems more competitive than BoR-FDTD in the general case, even when taking into account memory requirement. (See Figure 3).

III- Absorbing boundary conditions

The absorbing boundary conditions created for AS-TLM are based on a non-unified formulation. This kind of algorithm ensures stability of the ABCs by a coupling between TLM and FDTD [9]. Hence, the computational domain is modeled with AS-TLM and the PML layer is performed using BoR-FDTD. Coupling is achieved by performing interpolations as described in [9] for the 3D case. The first step of this approach is shown in Figure 4.

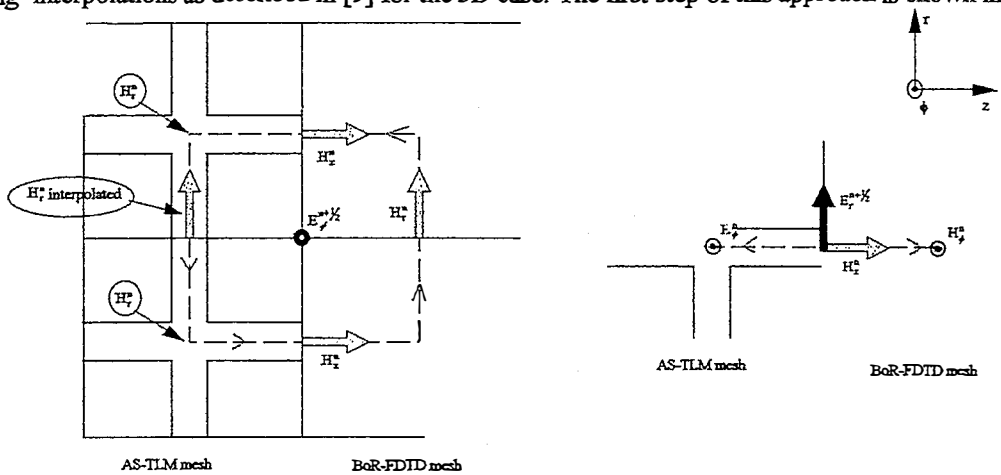

(a) **(b)**

Figure 4. First coupling step (from AS-TLM to BoR-FDTD).
(a) Calculating E_ϕ, **(b)** Calculating E_r at the interface.

The second step (from AS-TLM to BoR-FDTD) is straightforwardly performed as in [9]. It is important to notice that only two interpolations are needed instead of four in the 3D case. This feature insures better coupling performances. The algorithm is then tested in a circular waveguide where reflection on the interface is calculated. Results are reported in Figure 5. The coupling is excellent since the reflection coefficient with a coarse mesh is lower than -50 dB on the TE_{11} single-mode bandwidth.

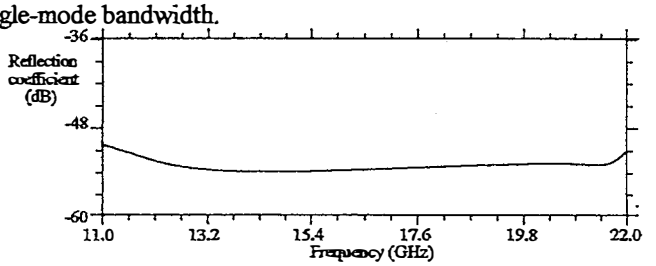

Figure 5. Reflection coefficient between AS-TLM and BoR-FDTD in a cylindrical waveguide excited with TE_{11} mode.

From a memory requirement point of view, anisotropic PML [10] were selected and adapted to the BoR-FDTD algorithm in an original manner. This PML formulation is governed in the frequency domain by equations of the following type:

$$\left(\nabla \wedge \vec{H}\right)_i = j\omega\varepsilon_r\varepsilon_0 \frac{s_j s_k}{s_i} E_i \qquad \text{with} \qquad s_i = \alpha_i\left(1+\frac{\sigma_i}{j\omega\varepsilon_r\varepsilon_0}\right) \quad \text{and} \quad (i,j,k) \in \{r,\phi,z\} \qquad (7)$$

where σ_i is the classical PML loss term (for propagating waves absorption) and α_i add to evanescent waves some damping. By manipulating (7) in the frequency domain, we obtain in the time domain:

$$\left(\nabla \wedge \vec{H}\right)_i = \frac{\alpha_j\alpha_k}{\alpha_i}\left[\varepsilon_r\varepsilon_0 \frac{\partial E_i}{\partial t} + \left(\sigma_k+\sigma_j-\sigma_i\right)E_i + F_i\right] \qquad (8)$$

$$\text{with:} \quad \varepsilon_r\varepsilon_0 \frac{\partial F_i}{\partial t} + \sigma_i F_i = \gamma_i E_i \qquad \text{and} \qquad \gamma_i = \left(\sigma_j\sigma_k - \sigma_i\left(\sigma_k+\sigma_j-\sigma_i\right)\right) \qquad (9)$$

From (8), it is remarkable that the only difference compared to classical Maxwell's equations is a source term and a loss one. Its implementation is straightforward: discretizing (9) leads to:

$$F_i^{(n+1/2)} = \Gamma_i^2 E_i^{(n+1/2)} + \Gamma_i^2 E_i^{(n-1/2)} + \Gamma_i^1 F_i^{(n-1/2)} \qquad \text{with:} \quad \Gamma_i^1 = \frac{\left(1-\frac{\sigma_i\Delta t}{2\varepsilon_0\varepsilon_r}\right)}{\left(1+\frac{\sigma_i\Delta t}{2\varepsilon_0\varepsilon_r}\right)} \;,\; \Gamma_i^2 = \frac{\gamma_i\Delta t}{2\left(1+\frac{\sigma_i\Delta t}{2\varepsilon_0\varepsilon_r}\right)} \qquad (10)$$

Equation (10) is injected in (8), that allows one to compute the electric field. The source term is then updated with (10). The only extra memory requirement is due to the F_i storage. In the case of an uniaxial medium, only two of them are required. In the general case 6 values are needed. Performances of this algorithm will be shown with antennas applications.

IV- Conclusion

A class of new TLM nodes was presented for the analysis of axially symmetric structures (AS-TLM). Performances in term of time step and memory make this method more competitive than the equivalent FDTD method (BoR-FDTD). Since PML layers are not mature in TLM (instabilities), anisotropic PML layers are used with a non-unified algorithm. Excellent performance of the coupling between AS-TLM and BoR-FDTD was established. Further applications will be shown especially a class of corrugated horn antennas.

References

[1] S. Le Maguer and M. M. Ney "Efficient TLM procedure for characterization of guiding structures with axial symmetry and arbitrary radial profile", *PIERS Proceedings*, 8-12 Jul. 1996, Innsbruck, pp 334.

[2] P.B. Johns, "A symmetrical condensed node for the TLM method," *IEEE Trans. MTT*, vol. 35, n°4, pp. 370-377, April 1987.

[3] A. Taflove, "The finite-difference time-domain method," *Computational Electrodynamics*, Artech House, Boston-London, Chap. 12, 1995.

[4] Y. Chen, R. Mittra and P. Harms, "Finite-difference time-domain algorithm for solving Maxwell's equation in rotationally symmetric geometries," *IEEE MTT*, vol. 44, n°6, pp 832-839, June 1996.

[5] N.Peña and M.M.Ney, "A general formulation of a three-dimensional TLM condensed node with the modeling of electric and magnetic losses and current sources," *ACES 96 conference proceedings*, pp.262-269, 1996.

[6] N.Peña and M.M.Ney, "A general two dimensional TLM hybrid node formulation based on Maxwell's integral equations," *ACES 96 conference proceedings*, pp.254-261, 1996.

[7] H. Jin and R. Vahldieck, "Direct derivations of TLM symmetrical condensed node and hybrid symmetrical condensed node from Maxwell's equations using centered differencing and averaging," *IEEE Trans. MTT*, vol. 42, n°12, pp. 2554-2561, Dec. 1994.

[8] V. Trenkic, C. Christopoulos and T.M. Benson, "Simple and elegant formulation of scattering in TLM nodes," *Electronics Letters*, vol. 29, n°18, pp. 1651-1652, Sept. 1993.

[9] N. Pena and M. M. Ney, "Absorbing boundary conditions using perfectly matched layer (PML) technique for 3D-TLM simulations," *IEEE Trans. MTT.*,vol. 45, n°10, 1997.

[10] S.D. Gedney,"An anisotropic perfectly matched layer absorbing medium for the truncation of FDTD lattices," *IEEE Trans. AP*, vol.44, n°12, Dec. 1996, pp.1630-1639.